DSMC SIMULATIONS OF OREX ENTRY CONDITIONS

James N. Moss, Roop N. Gupta, Joseph M. Price
(Aerothermodynamics Branch, NASA Langley Research Center, Hampton, Virginia 23681-0001, USA)

ABSTRACT: Results of direct simulation Monte Carlo (DSMC) solutions are presented for the Japanese Orbital Reentry Experiment (OREX) vehicle, a 50° half-angle spherically blunted cone with a nose radius of 1.35 m and a base diameter of 3.4 m. The flow conditions simulated are those for entry into the Earth's atmosphere at a nominal velocity of about 7.4 km/s and zero incidence. Calculations are made for the higher altitude portion of entry, encompassing the transitional flow regime (altitudes of 200 to 80 km). Comparisons with flight measured values are made for axial acceleration, surface pressure, and stagnation point heating.

1 INTRODUCTION

On February 4, 1994, the Orbital Reentry Experiment (OREX) was launched into Earth orbit by the H-II rocket with a successful probe reentry. OREX is the forerunner of a series of three flight experiments planned as part of the development program for Japan's unmanned space shuttle called HOPE. References 1 to 3 provide an indication of the scope and quality of the basic data obtained from OREX. Aerothermodynamic measurements were made with the objective of providing a data base that can be used to establish the creditability of computational design tools for space transportation systems. OREX was a 50° spherically blunted cone with a 1.35 m nose radius of curvature and a base diameter of 3.4 m. Measurements made in the 120 to 80 km altitude range cover much of the transitional flow regime. Measurements at these altitudes include the temperature response of several thermal protection materials, surface pressure, acceleration, and electron number density.

One motivation for comparing with the OREX data is that the inferred surface heating rate data are potentially unique for altitudes above about 95 km. Unlike the Shuttle Orbiter which is an operational vehicle, OREX was enclosed in a protective fairing during launch thereby negating the requirement for waterproofing the thermal protection materials. Consequently, the OREX thermal protection system should not produce some of the outgasing products and reduction in heating that would be common for the Orbiter during the initial heat pulse. The initial entry heating reported for OREX exhibits a behavior that is characteristic of a nonblowing surface whereas that evident for the Orbiter data might be explained in terms of outgasing (see Fig. 11 of Ref. 4).

The higher altitude portion of the OREX entry is the focus of the present study where the direct simulation Monte Carlo (DSMC) method of Bird[5] is used to calculate flow field and surface quantities of the OREX forebody. Calculations are made for altitudes of 200 km to 80 km. This altitude range encompasses the transitional flow regime in that the freestream Knudsen number ranges from 58 to 0.0009. Presented are comparisons of DSMC results with calculations made with a Navier Stokes solver[6] and a viscous shock layer code[7] and flight inferred results for axial acceleration, surface pressure, and stagnation point heating.

2 PROBLEM DEFINITION

2.1 Computational Method

The 2D/axisymmetric DSMC method of Bird[5] was used in the present study to calculate the forebody flow about the OREX vehicle. The DSMC method provides a capability of simulating flows across the complete flow spectrum of continuum to free molecular flows as utilized in the present study. Freestream quantities used in the present calculations are included in Table 1. As discussed in Ref. 7, the atmospheric properties

below 90 km are those given by Yamamoto[3, 6] while those above 90 km are from Jacchia[8] for an exospheric temperature of 1200 K.

Molecular collisions are simulated using the variable hard sphere (VHS) molecular model (Ref. 5). Energy exchange between kinetic and internal modes is controlled by the Larsen-Borgnakke[9] statistical model. For this study, simulations are performed using a reacting gas model with five chemical species while considering energy exchange between translational, rotational, and vibrational modes. For the diatomic molecules, a rotational relaxation collision number of 5 and a vibrational relaxation collision number of 50 were used.

For the gas surface interactions, the surface is assumed to be diffuse with full thermal accommodation and finite catalytic. The surface temperature distributions were obtained from Ref. 6 for altitudes less than 105 km where Navier-Stokes solutions for the flowfield were coupled with a material response code as described in Ref. 3. Above 105 km, the surface temperature was assumed constant at a value of 331.8 K.

2.2 OREX Vehicle

The OREX vehicle (Fig. 1) is a spherically blunted cone having a 50-deg half angle and a nose radius of 1.35 m. The shoulder corner radius is 0.1 m and the base diameter is 3.4 m. At entry, the vehicle weighed 761 kg.

The exposed forebody of OREX consisted of thermal protection materials that have been developed and are being assessed for use on Japan's unmanned space shuttle called HOPE. The nose cap was a monocoque carbon-carbon structure having a thickness of 4 mm. Surrounding the carbon-carbon hot structure were twenty-four carbon-carbon tiles 1.5 mm in thickness. Both the carbon nose and tiles are made from the same carbon-carbon mix. Ringing the carbon-carbon tiles are some 230 ceramic tiles made of silicon-oxide and aluminum-oxide fibers connected to OREX's aluminum honeycomb shell. The ceramic tiles were 20 mm in thickness.

Flight data for which comparisons are made with DSMC calculations are the inferred heating rates extracted from the back surface temperature measurements made at the nose cap stagnation point, the high-altitude and mid-altitude pressure sensors connected to inlets through the ceramic tiles, and the vehicle axial acceleration obtained from a micro-g accelerometer mounted along the vehicle symmetry axis. More detail concerning the flight measurements can be found in Refs. 1 through 3.

3 RESULTS

Figure 2 presents calculated results where the stagnation heating rate and drag quantities are shown as a function of altitude. Both the total drag coefficient and its pressure component are presented, demonstrating the large contribution of frictional drag in the transitional regime. The calculated results approach the free molecular value (C_D = 2.11) at high altitudes and the Mach 7 air wind tunnel results[2] (C_D = 1.19) at low altitudes. The present calculations cover altitudes down to 79.9 km where the calculated stagnation point heating is 36 percent of the peak heating which occurs at 63.6 km (7461.5 s) as shown in Fig. 3.

3.1 Stagnation-Point Heating

Results of temperature measurements have been reported in Refs. 1 through 3 for the carbon-carbon nose cap as well as the carbon and ceramic tiles. Less information is currently available concerning flight inferred heating rates. Consequently, the present comparisons will focus on the stagnation-point results for the carbon-carbon nose cap.

Agreement between calculated and measured stagnation-point heating rates is fair. Figure 3 presents the flight inferred stagnation-point heating rate results as a function of time from launch of OREX. Continuum results obtained with viscous shock layer (VSL)[7] and Navier-Stokes[6] solutions are shown for altitudes of 105 km to 48.4 km. The NS results are for a no-slip and a non-catalytic surface. The DSMC results shown for 105 to 79.9 km include the same finite catalytic wall boundary condition as used in the VSL calculations; however, the finite catalytic and non-catalytic boundary conditions yield essentially the same results over this altitude range (see Ref. 7). Inclusion of the slip boundary conditions at higher altitudes yield substantially lower heating rates for the VSL solution as is discussed in Ref. 7.

The heating rates are inferred from the temperature measurements made on the back surface of a carbon-carbon material. As additional data are reported, opportunities will exist for comparing calculated and measured results at various locations along the forebody.

A useful way of assessing the heat transfer results is to express the data in terms of the heat transfer coefficient, defined herein as $C_H = 2q/\rho_\infty V_\infty^3$. Figure 4 presents this data as a function of altitude for both the DSMC calculations and the inferred flight data. There are differences in the magnitudes up to 35 percent, but the general trends are consistent. The fact that both data sets have the correct qualitative features (namely, C_H increasing with rarefaction and approaching 1.0 in the free molecular limit) and are in fair quantitative agreement suggests that this set of evolving experimental data may be unique for the transitional flow regime. The OREX data exhibits a behavior that is characteristic of a nonblowing surface, whereas that evident for the Orbiter data might be explained in terms of outgasing (see Fig. 11 of Ref. 4 where the inferred C_H value is much less than the calculated value for altitudes > 95 km).

3.2 Surface Pressure

As described in Ref. 2, two pressure measurements at different radial and circumerential locations along the conical portion of the forebody were made during the OREX reentry where the inlet systems consisted of orifice/tube/cavity arrangements mounted flush with the external surface. One sensor provided data from high altitudes to about 75 km with a four-decade capacitative type transducer, referred to as the high altitude pressure sensor. The second sensor, referred to as the middle altitude pressure sensor was calibrated for the altitude range of about 80 to 40 km. The measured and calculated results indicate that the pressures at the two orifice inlet locations are approximately the same.

Figure 5 presents the pressure measurements (from Ref. 2) showing results from both pressure sensors as a function of altitude. The overlap between the high altitude and middle altitude sensor output around 80 km is shown to be very good. Since the two pressure sensors were displaced circumferentially (see Ref. 2), the overlap around 80 km altitude provides additional information concerning the orientation of OREX at this altitude.

Also shown in Fig. 5 is the calculated surface pressure (high altitude sensor location) which agrees very well with the measured results for altitudes below about 95 km. For altitudes greater than 95 km, the calculated surface pressure and the measured pressure diverge with increasing altitude. This behavior is qualitatively correct due to the highly nonequilibrium state--translational, rotational, vibrational, and chemical--that exists at the orfice inlet and along the tube connection to the pressure transducer. This well known behavior has been demonstrated[10] using the DSMC method to relate inlet tube pressure to the external surface pressure for the nose region of the Shuttle Orbiter during reentry. As shown in Fig. 12 of Ref. 10, the pressure inside an inlet tube can become a small fraction of the surface pressure with increasing rarefaction. Consequently, additional analyses would be required to relate the "measured pressure" at high altitudes with the calculated surface pressures.

3.3 Acceleration

Tabulated values of the drag coefficient are included in Table 1 and the results are shown in Fig. 2 as a function of altitude. Knowing the drag coefficient, acceleration as a function of altitude can be generated (Fig. 6) for an entry mass of 761 kg (assumed constant) and a cross-sectional area of 9.0792 m^2. When the flight data is extracted from Fig. 15 of Ref. 2 (fidelity of comparison would be improved if tabulated flight data were available), the agreement with calculated values is very good considering the potential atmospheric variability that OREX could have encountered relative to the atmosphere used in the calculations.

Independent DSMC calculations by Koura for the drag coefficient and acceleration are included in Ref. 2 for a Knudsen number range of 0.01 to 10. Koura's values for drag coefficient differ from the present calculations; however, the reason for the discrepancy is not known.

4 CONCLUDING REMARKS

Comparisons of DSMC solutions with OREX measured or inferred results are made for acceleration, surface pressure, and stagnation-point heating rates. In general, the comparisons show good agreement. For acceleration, the agreement is exceptionally good. Calculated and measured surface pressure values are in good quantitative agreement for the lower altitudes but depart with increasing altitude as they should due to the high degree of nonequilibrium that exists at and within the inlet system used for the "measured pressure". Agreement for calculated and inferred flight heating rates is fair to good.

The overall good correspondence of flight and calculated results is very encouraging. Furthermore, the flight inferred heat transfer rate data may be unique for most of the transitional flow regime in that it exhibits correct qualitative behavior with increasing rarefaction. As additional refinements in data extraction/definition are made and additional forebody heating rate information is published, an enhanced aerothermodynamic data base is expected to evolve from the OREX activity.

REFERENCES

[1] NAL/NASDA Joint Research Report. OREX, March 1995 (in Japanese).

[2] Inouye, Y. OREX Flight--Quick Report and Lessons Learned. 2nd European Symposium on Aerothermodynamics for Space Vehicles, ESTEC, November 1994.

[3] Yamamoto, Y. and Yoshioka, M. CFD and FEM Coupling Analysis of OREX Aerothermodynamic Flight Data. AIAA Paper 95-2087.

[4] Moss, J. N. and Bird, G. A. Direct Simulation of Transitional Flow for Hypersonic Re-entry Conditions. *Progress in Astronautics and Aeronautics: Thermal Design of Aeroassist Orbital Vehicles*, edited by H. F. Nelson, vol. 96, 1985, pp. 113-139.

[5] Bird, G. A. *Molecular Gas Dynamics and the Direct Simulation of Gas Flows*. Clarendon Press, Oxford, 1994.

[6] Yamamoto, Y. Private communications, National Aerospace Laboratory, Japan, December 1995.

[7] Gupta, R. N., Moss, J. N., and Price, J. M. Assessment of Thermochemical Nonequilibrium and Slip Effects for Orbital Reentry Experiment (OREX). AIAA Paper 96-1859.

[8] Jacchia, L. G. Thermospheric Temperature, Density, and Composition: New Models. Smithsonian Astrophysical Observatory, Cambridge, MA, Special Rept. 375, March 1977.

[9] Borgnakke, C. and Larsen, P. S. Statistical Collision Model for Monte Carlo Simulation of Polyatomic Gas Mixtures. *Journal of Computational Physics*, vol. 18, no. 4, 1975, pp. 405-420.

[10] Moss, J. N. and Bird, G. A. Monte Carlo Simulations in Support of the Shuttle Upper Atmoshperic Mass Spectrometer Experiment. *Journal of Thermophysics and Heat Transfer*, vol. 2, no. 2, 1988, pp. 138-144, (also AIAA Paper No. 85-0968, June 1985).

Table 1. Flight Conditions and Results of DSMC Simulations

Altitude, km	Velocity, m/s	Number Density, m^{-3}	T_∞, K	Mole Fractions X_{O2}	X_{N2}	X_O	T_W[a], K	Kn_∞	C_D	Stagnation heating, kW/m^2
200.0	7400.0	8.9996×10^{15}	1025.8	0.0315	0.4548	0.5138	331.8	5.79×10^{1}	2.085	6.93×10^{-2}
170.0	7400.0	2.2700×10^{16}	891.5	0.0435	0.5482	0.4083	331.8	2.22×10^{1}	2.066	1.76×10^{-1}
150.0	7412.0	5.3055×10^{16}	733.4	0.0546	0.6156	0.3298	331.8	9.10×10^{0}	2.016	4.00×10^{-1}
135.0	7422.0	1.3149×10^{17}	546.2	0.0659	0.6716	0.2625	331.8	3.46×10^{0}	1.957	1.08×10^{0}
125.0	7431.0	3.0598×10^{17}	433.4	0.0768	0.7117	0.2115	331.8	1.40×10^{0}	1.899	2.46×10^{0}
120.0	7439.0	5.2130×10^{17}	367.8	0.0845	0.7327	0.1828	331.8	7.90×10^{-1}	1.867	4.13×10^{0}
115.0	7440.0	9.8562×10^{17}	304.4	0.0978	0.7539	0.1484	331.8	4.00×10^{-1}	1.824	7.90×10^{0}
110.0	7445.0	2.1246×10^{18}	247.4	0.1232	0.7704	0.1064	331.8	1.77×10^{-1}	1.741	1.54×10^{1}
105.0	7451.0	5.0515×10^{18}	211.0	0.1528	0.7815	0.0657	331.8	7.18×10^{-2}	1.616	3.20×10^{1}
101.1	7454.6	1.0326×10^{19}	196.9	0.1726	0.7839	0.0435	401.5	3.46×10^{-2}	1.502	5.33×10^{1}
96.8	7456.3	1.9812×10^{19}	190.3	0.1884	0.7863	0.0253	485.2	1.79×10^{-2}	1.407	7.45×10^{1}
92.8	7454.1	4.0845×10^{19}	188.3	0.2025	0.7881	0.0094	586.1	8.64×10^{-3}	1.326	9.44×10^{1}
88.4	7444.3	8.9890×10^{19}	186.9	0.2125	0.7875	0.0000	686.9	3.92×10^{-3}	1.274	1.13×10^{2}
84.0	7415.9	2.2780×10^{20}	188.9	0.2375	0.7625	0.0000	785.1	1.55×10^{-3}	1.241	1.32×10^{2}
79.9	7360.2	3.8380×10^{20}	198.6	0.2375	0.7625	0.0000	878.4	9.30×10^{-4}	1.231	1.50×10^{2}

[a]CFD inferred stagnation surface temperatures of Yamamoto[6] for altitudes of 105 km and less.

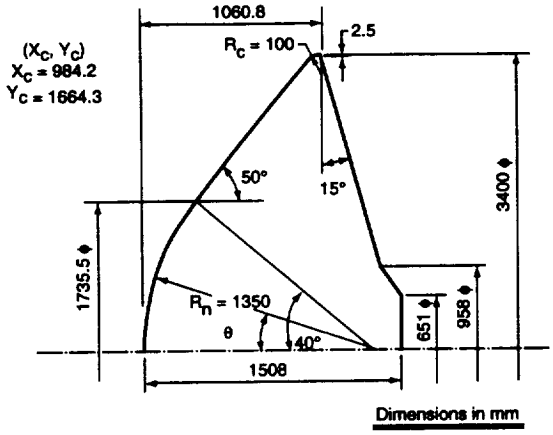

Fig 1. OREX configuration.

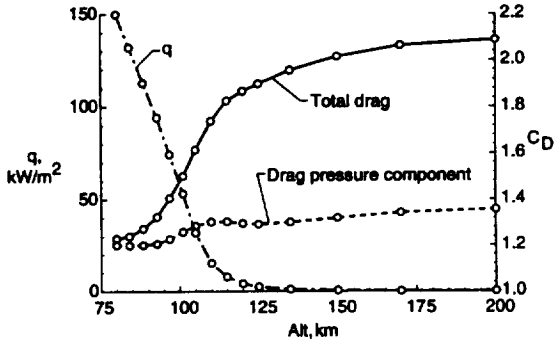

Fig. 2. Calculated stagnation heating and drag for OREX.

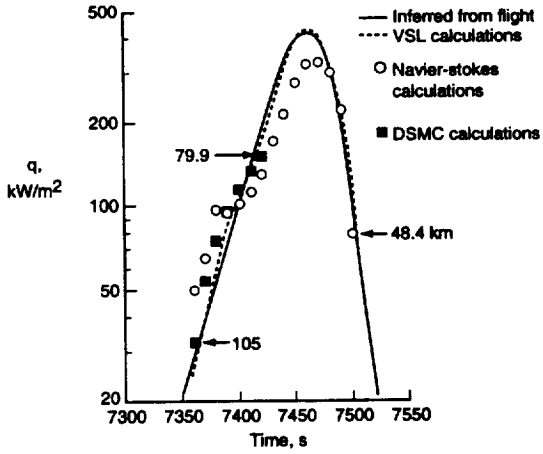

Fig 3. Comparison of flight inferred[3] stagnation-point heating rates with calculations using VSL[7], NS[6], and DSMC.

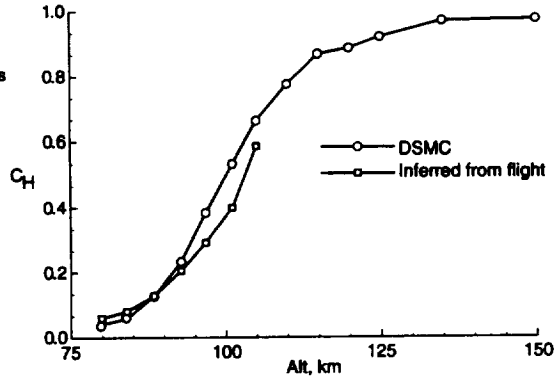

Fig. 4. Comparison of flight inferred[3] stagnation-point heating rate coefficient with DSMC results.

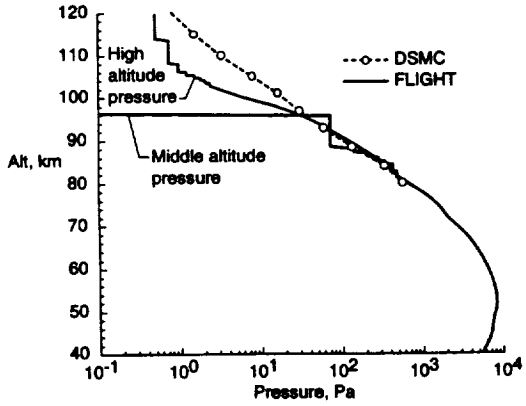

Fig. 5. Comparison of calculated and measured[2] surface pressures on forebody cone.

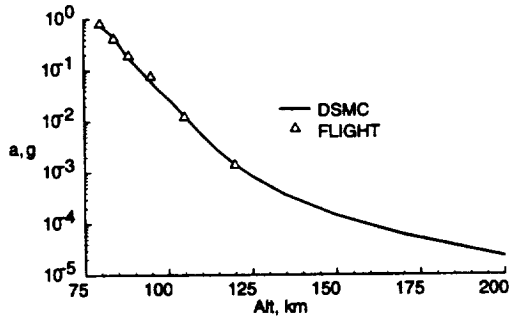

Fig. 6. Comparison of calculated and measured[2] OREX axial acceleration.